

LANGLEY SUB-LIBRARY

~~RESTRICTED~~

NM A6430

110
Douglas
BTD-1/2

FEB 21 1947



NACA

RESEARCH MEMORANDUM

for the

Bureau of Aeronautics, Navy Department

COMPARISON OF WIND-TUNNEL PREDICTIONS WITH FLIGHT
MEASUREMENTS OF THE LONGITUDINAL-STABILITY
AND -CONTROL CHARACTERISTICS OF A
DOUGLAS BTD-1 AIRPLANE

FOR REFERENCE

Mortimer Bunnell and Noel K. Delany

Ames Aeronautical Laboratory
Moffett Field, Calif.

NOT TO BE TAKEN FROM THIS ROOM

~~CLASSIFIED DOCUMENT~~

CONTAINS PROPRIETARY
INFORMATION

This document contains classified information affecting the National Defense of the United States within the meaning of the Espionage Act, USC 50:31 and 32. Its transmission or the revelation of its contents in any manner to an unauthorized person is prohibited by law. Information so classified may be imparted only to persons in the military and naval Services of the United States, appropriate civilian officers and employees of the Federal Government who have a legitimate interest therein, and to United States citizens of known loyalty and discretion who of necessity must be informed thereof.

TECHNICAL
EDITING
WAIVED

**NATIONAL ADVISORY COMMITTEE
FOR AERONAUTICS**

WASHINGTON
FEB 13 1947

NACA LIBRARY
LANGLEY MEMORIAL AERONAUTICAL
LABORATORY
Langley Field, Va.

~~RESTRICTED~~



NATIONAL ADVISORY COMMITTEE FOR AERONAUTICS

RESEARCH MEMORANDUM

for the

Bureau of Aeronautics, Navy Department

COMPARISON OF WIND-TUNNEL PREDICTIONS WITH FLIGHT

MEASUREMENTS OF THE LONGITUDINAL-STABILITY

AND -CONTROL CHARACTERISTICS OF A

DOUGLAS BTD-1 AIRPLANE

By Mort V. Bunnell and Noel K. Delany

SUMMARY

Low Mach number longitudinal-stability and -control characteristics as predicted by use of wind-tunnel data from a powered 3/16-scale model are compared with flight-test measurements of a Navy BTD-1 airplane. The accuracy of the wind-tunnel data and the discrepancies involved in attempting to correlate with flight data are discussed and analyzed.

The comparison showed that wind-tunnel predictions were, in general, in good agreement with flight-test data. The predicted values were for the most part sufficiently accurate to show the satisfactory and unsatisfactory characteristics in the preliminary design stage and to indicate possible methods of improvement. The discrepancies which did occur were attributed principally to physical dissimilarities between model and airplane and the inability to determine accurately the flight power conditions. The effect of Mach number was considered negligible since the maximum flight-test value was about 0.5. In order to simulate more closely the flight conditions and hence obtain more accurate data for predictions, it appears desirable to perform large-scale tests of unorthodox control surfaces such as the sealed vaned elevators with which the airplane was equipped.

INTRODUCTION

The flying qualities of various types of airplanes have been predicted during the last few years from wind-tunnel measurements of powered scale models. In the past, when the predictions have indicated unsatisfactory stability and control characteristics, wind-tunnel data have been used as a guide in the redesign of the

~~RESTRICTED~~

airplane. The NACA has undertaken an investigation to study the reliability of this prediction procedure by a detailed comparison of flight and wind-tunnel data. (See references 1 and 2.)

As part of this correlation program, flight-test data on the longitudinal-stability and -control characteristics of a Douglas BTD-1 airplane are compared in this report with the results of tests at low Mach number of a powered 3/16-scale model in the Ames 7- by 10-foot wind tunnel. The results are confined to the following important characteristics which are most suitable for prediction and correlation: static longitudinal stability, elevator control in maneuvering flight, and elevator control in landing.

The wind-tunnel data were converted into the usual flight-test units of airspeed, normal acceleration, and elevator angle and control force, and compared with the flight-test results. In order to analyze the data in more fundamental form, basic aerodynamic derivatives were estimated from flight-test results and compared with the wind-tunnel derivatives.

DESCRIPTION OF THE AIRPLANE

The BTD-1 airplane is a torpedo dive bomber intended for use aboard aircraft carriers. It is a single-engine, single-place, midwing monoplane equipped with a retractable tricycle landing gear and combination fuselage and wing dive brakes. General characteristics of the airplane, wing, and horizontal-tail-plane dimensions, and dimensions of the flap, elevator, and elevator tab are listed in tables I, II and III, respectively. Figure 1 shows the airplane as instrumented for flight tests and figure 2 is a three-view drawing. Figure 3 gives details of the horizontal-tail surfaces.

No correlation was attempted with the dive brakes open due to large differences between the airplane and model dive brakes. In order to simulate the model, the wing dive brakes on the airplane were removed, the openings faired over, and the wing-fold gaps sealed. The fuselage dive brakes were locked in the closed position. Figure 4 gives the force characteristics of the spring-loaded elevator system as measured on the ground during slow movement of the control column. The elevator on the airplane was connected with the flap system in such a manner that larger up-elevator deflections were obtained when the flaps were down. The kinematics of this system are presented in figure 5.

DESCRIPTION OF THE MODEL

The 3/16-scale powered model of the Douglas BTD-1 airplane as tested in the Ames 7- by 10-foot wind tunnel is shown in figure 6. Power was supplied by an electric motor which drove a 3/16-scale

four-blade propeller. A propeller spinner was used in all the model tests. The model elevator was equipped with a nose seal and a fixed vane (fig. 3). No elevator tabs were installed. A detailed view of the model wing flaps is presented in figure 7. The cut-out spaces for the wing flaps varied slightly from those of the airplane.

AIRPLANE INSTRUMENT INSTALLATION

Standard NACA instruments were used to record photographically, as a function of time, quantities from which the following variables could be obtained: airspeed, normal acceleration, altitude, and applied elevator control force. The engine-operation data were read from the service instruments in the airplane. The mechanical-type elevator-position recorder was attached directly to the elevator control horn. Both strain-gage and mechanical-type instruments were used in the measurement of elevator-control forces. A free-swivelling airspeed head was mounted 3 feet inboard from the wing tip on a boom that extended approximately 4-1/2 feet ahead of the wing leading edge. (See fig. 1.) Throughout this report the values of indicated airspeed were computed from the airspeed formula (corrected for compressibility) commonly used in the calibration of standard airspeed indicators.

$$V_i = 1703 \left[\left(\frac{H-p}{29.92} + 1 \right)^{0.286} - 1 \right]^{\frac{1}{2}}$$

where

H free stream total pressure in inches of mercury
p free stream static pressure in inches of mercury

COEFFICIENTS AND SYMBOLS

The coefficients and symbols used in this report are defined as follows:

C_L lift coefficient (L/qS)
 C_m pitching-moment coefficient about the center of gravity
 ($M/qS \text{ M.A.C.}$)
 C_{m_0} pitching-moment coefficient about the center of gravity
 at zero lift coefficient
 $C_{m\delta_e}$ the rate of change of pitching-moment coefficient with
 elevator angle $(\partial C_m / \partial \delta_e) C_L \delta_t$ at constant lift coefficient
 and tab angle

$C_{m_{CL}}$	the rate of change of pitching-moment coefficient with lift coefficient $(\partial C_m / \partial C_L)_{\delta_o \delta_t}$ at constant elevator and tab angle
C_h	elevator hinge-moment coefficient $(H/qS_e \bar{c}_e)$
$C_{h_{\delta_e}}$	the rate of change of elevator hinge-moment coefficient with elevator angle $(\partial C_h / \partial \delta_e)_{C_L \delta_t}$ at constant elevator tab angle
$C_{h_{\delta_t}}$	the rate of change of elevator hinge-moment coefficient with tab angle $(\partial C_h / \partial \delta_t)_{C_L \delta_e}$ at constant lift coefficient and elevator angle
$C_{h_{CL}}$	the rate of change of elevator hinge-moment coefficient with lift coefficient $(\partial C_h / \partial C_L)_{\delta_o \delta_t}$ at constant elevator and tab angle
T_c	thrust coefficient $(T/\rho V^2 D^2)$
δ_e	elevator angle, degrees
δ_t	tab angle, degrees
δ_{t_0}	tab angle to trim to zero control force, degrees
S	wing area, square feet
M.A.C.	mean aerodynamic chord of the wing, feet
S_e	elevator area aft of the hinge line, square feet
\bar{c}_e	elevator root-mean-square chord aft of the hinge line, feet
D	propeller diameter, feet
F_e	elevator control force, pounds
L	lift, pounds
W	airplane weight, pounds
M	pitching moment about the center of gravity, foot-pounds
H	elevator hinge moment, foot-pounds
T	net thrust of the propeller, pounds
g	acceleration of gravity (32.2 ft/sec ²)

- A_z the ratio of the net aerodynamic force along the airplane Z-axis (positive when directed upward) to the weight of the airplane
- q dynamic pressure ($\frac{1}{2}\rho V^2$), pounds per square foot
- ρ air density, slugs per cubic foot
- V true airspeed, feet per second
- V_i correct indicated airspeed, miles per hour

TESTS

As mentioned in the introduction, this report deals with static-longitudinal stability, elevator control in turning flight, and elevator control in landing. The following is a brief description of the tests and methods of computation.

Flight Tests

The flight tests were performed at two center-of-gravity positions (approximately 0.264 and 0.309 M.A.C. flap and gear up) and although there were small variations in weight due to ballast and fuel consumption, the average gross weight of the airplane during all tests was approximately 18,000 pounds. Due to engine restrictions for high blower operation, all tests were performed at a pressure altitude of less than 6000 feet. The maximum test Mach number was approximately 0.5, while the Reynolds number varied from 8×10^6 to 26×10^6 . The following chart describes the various test configurations:

Condition	Position			Power		
	Flaps	Gear	Cowl flap	Manifold pressure (in. Hg)	Engine speed setting (rpm)	Brake horsepower
Glide	Up	Up	Closed	15	2200	—
Power-on clean	Up	Up	Open	45	2400	2100
Landing	Full down	Down	Closed	Throttled	2400	—
Approach	Full down	Down	Closed	28	2400	1430

Static longitudinal-stability characteristics.— The variations of elevator angle and elevator control force (tab constant) with airspeed were obtained from short records taken in steady, straight, wings-level flight at various airspeeds for the four flight conditions and two center-of-gravity locations described previously. In addition, the variation of elevator control force with tab deflection was measured at several constant airspeeds in each condition. The slopes of the latter curves of the variation of elevator control force with tab deflection were used over the linear range to determine the flight variation of tab effectiveness $Ch\delta_t$ with lift coefficient.

The stick-fixed and stick-free neutral-point positions were derived from curves of elevator angle and tab angle for trim (cross-plotted from the stick-force tab-angle curves at zero force) as a function of lift coefficient. The slopes $d\delta_e/dC_L$ and $d\delta_{t_0}/dC_L$ were plotted as a function of center-of-gravity location. The locations for $d\delta_e/dC_L = 0$ ($C_m = 0$) and $d\delta_{t_0}/dC_L = 0$ ($C_m = 0$ and $C_h = 0$) were taken as the stick-fixed and stick-free neutral-point locations, respectively.

Elevator control in turning flight.— The variation of elevator angle and stick force with normal acceleration factor was measured in turning flight in the power-on clean condition. The airplane was first trimmed to zero stick force at each test speed in a wings-level steady-flight condition. Short records were taken (airspeed constant) at various acceleration factors (A_z). Due to structural limitations the maximum test in acceleration was limited to about 3g.

Elevator control in landing.— Landings were made at various touchdown airspeeds over a safe and feasible range. The tests were performed in the landing configuration (i.e., flaps down, gear down, and engine throttled) at both center-of-gravity positions. The elevator-tab setting was approximately the same as that used by the pilot in the flights to determine the static stability in the landing configuration.

Wind-Tunnel Tests

The wind-tunnel tests were made at dynamic pressures of 10 to 50 pounds per square foot, corresponding to model Reynolds numbers of 1.0×10^6 to 2.3×10^6 . As a compromise between high- and low-speed power-on flight conditions, the propeller-blade angle was set at 19° at the 0.75 radius station.

Basic data.— The data were first plotted as curves of lift coefficient C_L , pitching-moment coefficient C_m , and elevator hinge-moment coefficient C_h , as functions of thrust coefficient T_c for various constant angles of attack and elevator deflection.

The cross plots of these data were used to obtain the wind-tunnel curves of pitching-moment coefficient and hinge-moment coefficient as a function of lift coefficient. The test conditions are outlined in the following table:

Model configuration		Elevator angle (deg)	Tail incidence (deg)	Thrust coefficient
Flaps and gear	Propeller			
Up	Off	5 to -35	0.75	---
Up	On	5 to -15	.75	0 to 0.75
Up	On	0	4	0 to .75
Up	Off	0	4	---
Down	Off	5 to -30	.75	---
Down	On	5 to -30	.75	0
Down	On	5 to -15	.75	0 to .25
Down	On	5 to -10	.75	0 to .85
Down	On	0	4	0 to .85
Down	Off	0	4	---
Down ¹	On	0 to -35	.75	0 to .25

¹Ground board installed in wind tunnel for these tests.

Derivation of stability and control characteristics.

Reference 3 describes the methods used for computing variations of elevator control force and elevator angle with airspeed in steady, straight flight; elevator-angle and stick-force gradient required in turning flight; and the variation of elevator angle and control force with contact speed in landings. The data, used in the derivation of the landing characteristics, were obtained in the presence of a wind-tunnel ground board. The results were computed

for a gross weight of 18,000 pounds and for the center-of-gravity positions used in flight and noted on the figures. The kinematics of the control system (fig. 5) and the effect of a bungee (fig. 4) used in the computations were the values measured on the airplane.

RESULTS AND DISCUSSION

Static-Longitudinal-Stability Characteristics

The variations of elevator deflection and elevator control force with indicated airspeed for all configurations are presented in figures 8 to 11, inclusive. Figure 12 shows the variation of elevator angle with lift coefficient in the landing configuration.

Glide condition.— Figure 8 shows positive stick-fixed and stick-free stability over the speed range at both center-of-gravity positions. The quantitative agreement between flight and wind-tunnel data is good.

The stick-fixed stability (fig. 13(a)) as measured by the slopes of $d\delta_e/dV_1$ (or $d\delta_e/dC_L$) and neutral-point location are approximately the same. Analysis indicated that the differences in $d\delta_e/dV_1$ for the forward center-of-gravity location — more stable for flight at low speeds and for the wind tunnel at high speeds — are due primarily to the more negative wind-tunnel values of $C_{m\delta}$ and C_{mC_L} .

When elevator angle was plotted as a function of lift coefficient, greater down-elevator angles were obtained at $C_L = 0$ for the model than for the airplane, an indication of a more positive C_{m_0} for the model. This accounts in part for the absolute shift in the elevator-angle curves of figures 8 to 11. The C_{m_0} difference was also indicated in the other configurations, although its effect on the $\delta_e - V_1$ curves is sometimes obscured by differences in C_{mC_L} and $C_{m\delta}$. This difference in C_{m_0} indicates that the airplane may have had a more positive stabilizer setting than the model.

There is good agreement in the stick-force characteristics at the rear center-of-gravity location and fair agreement at the forward location, the flight curves having greater slopes in each case. The stick-free neutral-point location computed from the flight data is about 6 percent forward of the predicted value. (See fig. 13(a).) Although the flight tests indicate a more negative (i.e., less stable) value of Ch_{C_L} than the wind-tunnel tests, the force-curve slopes in figure 8 are greater for flight, due primarily to more negative flight values of Ch_{δ} . Some of the disagreement, especially with center of gravity forward, may be attributed to the different $d\delta_e/dV_1$ slopes. As shown in figure 8, better agreement was obtained when the flight elevator angles were used in the

wind-tunnel computations. Flight measurements show a large decrease in tab effectiveness with increasing lift coefficient (fig. 14). This tends to make the flight data more stable, especially at low speeds.

Power-on clean condition.— In figure 9 the wind-tunnel predictions and flight-test results show positive stick-fixed and stick-free stability over the speed range. Except for the greater flight stick forces at the forward center-of-gravity position, the agreement between flight and wind-tunnel data is good. The slope of elevator angle with velocity (fig. 9) and the neutral-point location (fig. 13(a)) and hence $C_{m_{CL}}$ and $C_{m_{\delta}}$ are approximately the same for the flight and wind-tunnel data. There is good agreement in the stick-force characteristics at the rear center-of-gravity position and fair agreement in the forward position, with the flight curves being more stable in each case. The stick-free neutral point for the wind tunnel was within about 2 percent M.A.C. of that measured in flight at low speeds. Analysis indicated the possibility of control-surface distortion in flight at speeds greater than 200 miles per hour, such that $C_{h_{CL}}$ and $C_{h_{\delta}}$ became more positive with increasing speed. The $C_{h_{CL}}$ effect predominated and increased the stable flight forces at high speeds causing a rapid rearward neutral-point movement, as indicated in figure 13(a).

Landing condition.— Figure 10 shows that in both the wind-tunnel predictions and flight-test results, positive stick-fixed and acceptable stick-free stability are present over the speed range.

The slopes of the elevator-angle curves are greater for flight than for the predicted values, especially at the forward center-of-gravity location. Analysis showed these differences were due primarily to a greater wind-tunnel elevator effectiveness (more negative $C_{m_{\delta}}$). A plot of elevator angle as a function of lift coefficient (fig. 12) indicates that the flight elevator effectiveness was very low at high lift coefficients and at the forward center-of-gravity location. It appeared that the elevator lost considerable effectiveness in flight at large deflections (greater than approximately 90° up). In establishing the stick-fixed neutral-point location, allowance was made for this loss in effectiveness. Figure 13(b) shows that the stick-fixed location was rearward of 0.40 M.A.C., and that flight and wind-tunnel data are in good agreement.

The elevator control forces are in good agreement at the rear center-of-gravity location and fair agreement at the forward location, with the curves obtained in flight being slightly more stable in each case. Figure 13(b) shows that the predicted stick-free neutral-point is about 0.06 M.A.C. aft of the flight location. Further analysis indicated that although $C_{h_{CL}}$ computed from flight data was more negative (less stable) than predicted by the wind-tunnel, the more

stable stick-force slopes as measured in flight are due for the most part to the more negative flight values of Ch_{C_L} .

Approach condition.— In figure 11 both the wind-tunnel predictions and the flight-test results indicate positive stick-fixed stability over the speed range, except at the rear center-of-gravity location where the elevator control forces are unstable at speeds below 105 miles per hour.

The stick-fixed stability as shown by the elevator-angle slopes at both center-of-gravity positions and the neutral-point locations (fig. 13(b)) is in good agreement throughout. The rapid forward movement of neutral-point location with increased lift coefficient indicates a sizeable destabilizing effect due to power.

The stick forces as determined by the wind tunnel are approximately the same as those measured in flight, while the predicted neutral-point location is about 0.02 M.A.C. aft of the flight-test location — an indication of a more positive flight Ch_{C_L} . The slight difference of the stick-force curves at low speeds for the forward center-of-gravity location is due for the most part to the more stable flight elevator-angle variation.

Longitudinal-Control Characteristics in Turning Flight

Excessive control-force gradients (greater than 12 or 15 lb/g) are shown in figures 15 and 16 for both flight and wind-tunnel tests at the forward center-of-gravity location, and for the rear location at the high speeds. An examination of the wind-tunnel results would lead to the conclusion that the elevator control-force gradient would be excessive at center-of-gravity locations forward of about 0.31 M.A.C. The flight results lead to the same conclusion for the lower speeds; however, the gradients are considerably greater than predicted at higher speeds. They are slightly less than predicted at the rear center of gravity at lower speeds. As would be expected from the good agreement in stick-fixed static longitudinal stability characteristics there is no large or consistent difference between the flight and wind-tunnel elevator-angle gradients.

Compared with the wind-tunnel results for 145 and 210 miles per hour, the larger flight variation of control-force gradient with center-of-gravity location and the more forward flight maneuvering-point location (fig. 16) indicate more negative flight values of Ch_{δ} and Ch_{C_L} , respectively. This conclusion agrees with the discussion given previously for the glide and power-on-clean static-stability data. At the highest test speed of 272 miles per hour, the flight variation of stick-force gradient with center-of-gravity location is less than at low speeds and is in better agreement with the predicted value, while the flight maneuvering point is rearward of the predicted location. This

indicates that the flight values of C_{hs} and C_{hCL} tend to become more positive at high airspeeds, a phenomena previously discussed in connection with the power-on-clean static-stability data.

Elevator Control in Landings

Figure 17 shows the wind-tunnel and flight-test data of elevator angle and elevator control force required in landings. For satisfactory control at the forward center-of-gravity location the elevator should be capable of holding the airplane off the ground at 1.05 V_{SL} . It is estimated that this would correspond to approximately 94 miles per hour, but due to the objectionable stalling characteristics of the BTD-1 airplane no attempt was made to land at less than 95 miles per hour. The wind-tunnel predictions indicate that at center-of-gravity locations forward of 0.27 M.A.C. elevator control would be marginal at speeds below 95 miles per hour. Under the same loading conditions the flight data indicate that the amount of elevator available is insufficient.

Comparison of the elevator-angle data of figure 17 with that of figure 10 indicates large ground effect at low speeds (approximately 12° at 95 mph) and the agreement between flight and wind-tunnel data is good. The difference in absolute values of elevator angle is due mainly to the larger elevator effectiveness and more positive C_{m_0} for the model, as previously discussed in connection with the glide configuration static-stability data.

The correlation of elevator control forces between the wind-tunnel and flight data is fair. The predicted values of elevator control force for low-speed landings (100 to 110 mph) range from 28 to 40 pounds for the test center-of-gravity range, compared to a desired maximum of 35 pounds. The corresponding flight values were greater than 45 pounds, and were considered excessive. The use of large down-tab angles would have resulted in a reduction of forces (estimated 10 lb change at 100 mph), but would have given large push forces in the approach. Due to the large number of variables involved, it is difficult to determine the reason for the difference between flight and predicted force values; however, it appears that the larger flight values are to a large extent due to more negative C_{hs} , as mentioned previously in the static-stability discussion.

Differences in Correlation

In attempting to correlate flight-test data of the BTD-1 airplane with data obtained in the Ames 7- by 10-foot wind-tunnel numerous difficulties were encountered. Due to the small scale of the model, some physical differences may be noted, such as the lack of elevator trim tabs and changes in the wing flap cut-outs. Also, distortion of the small vane on the lower surface of the model

elevator may be a reason for a discrepancy in the comparison of the elevator derivatives. This small vane may also be subject to large Reynolds number effects. It was determined from unpublished full-scale wind-tunnel data on file at the Laboratory that, due to leakage, the elevator seal used in flight was less effective than that tested in the 7- by 10-foot wind tunnel. This resulted in less negative $C_{m\delta}$ and more negative Ch_{C_L} values for flight. The airplane elevator fabric was excessively loose in comparison with other airplanes, and considerable fabric distortion was indicated at speeds above 200 miles per hour. Throughout all configurations a comparison of the elevator-angle curves determined from flight and wind-tunnel measurements shows an absolute displacement of about 2° which could be ascribed to the difference in elevator $C_{m\delta}$. Analysis indicated that this could result from a more positive flight stabilizer setting of about 0.3° . Additional possible errors due to control friction, the allowance for spring load in the elevator system, and changes in elevator-tab effectiveness made elevator-force correlation especially difficult. Although an effort was made to maintain definite power relations, some of the discrepancy noted in the landing and glide conditions may be caused by differences in the airplane and model $T_C - C_L$ relationship.

For all conditions the correlation for stick-fixed stability as measured by $d\delta_e/dV_1$ is fairly good, with the largest discrepancy being noted in the landing condition at the forward center-of-gravity location. This discrepancy is evidently caused by a large decrease of the elevator effectiveness in flight at large up-deflections. In wind-tunnel computations zero thrust coefficient was used for the power-off conditions; whereas in flight the propeller might have been operating at negative values.

The differences in the correlation of stick-free stability as measured by dF_e/dV_1 are the result of a number of varying factors. Small changes in $C_{m\delta}$, Ch_{C_L} , Ch_δ , and elevator-tab effectiveness give in some configurations large differences in the comparison of the stick-force slopes. The difference in the landing and glide conditions at the forward center-of-gravity location is due in part to the negligible change in tab effectiveness (computed for $T_C = 0$), with C_L and a less negative Ch_δ obtained from the wind-tunnel data. Again this change in Ch_δ may be caused by seal leakage, distortion effects and the propeller operating at a negative T_C value in flight.

CONCLUSIONS

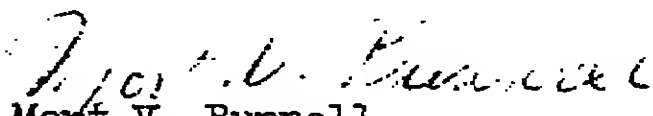
From the data presented in this report on the Navy BTD-1 airplane the following conclusions may be drawn with regard to the correlation of the data obtained in flight and that obtained in the Ames 7- by 10-foot wind tunnel:


1. The correlation of the wind-tunnel predictions with the longitudinal-stability and -control characteristics obtained in flight is qualitatively good. The wind-tunnel predictions indicated the same satisfactory or unsatisfactory characteristics that were obtained in flight for the critical conditions.

2. The wind-tunnel data are of sufficient accuracy to indicate the chief reasons for the unstable characteristics, and possible methods of improvement. However, there were sizeable quantitative differences in the flight and wind-tunnel elevator aerodynamic derivatives, due in large part to physical dissimilarities between the model and airplane (especially the control system), imperfect matching of power conditions, and flight control-surface distortion.


3. Large-scale wind-tunnel tests of the tail surfaces in which flight conditions are more closely duplicated would no doubt yield aerodynamic data which would permit better quantitative predictions of flight characteristics, especially for an unorthodox control surface such as the sealed elevator with a nose vane as installed on the BTD-1 airplane.

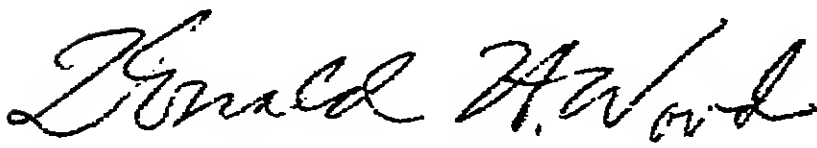
Ames Aeronautical Laboratory,
National Advisory Committee for Aeronautics,
Moffett Field, Calif.


Mort V. Bunnell,
Aeronautical Engineer.


Noel K. Delany,
Aeronautical Engineer.

Approved:


John F. Parsons,
Aeronautical Engineer.


Donald H. Wood,
Aeronautical Engineer.

REFERENCES

1. Delany, Noel K., and Kauffman, William M.: Correlation of Wind-Tunnel Predictions with Flight Tests of a Navy PV-1 Airplane. I - Longitudinal-Stability and -Control Characteristics. NACA MR No. A5D04, 1945.
2. Kayten, Gerald G., and Koven, William: Comparison of Wind-Tunnel and Flight Measurements of Stability and Control Characteristics of a Douglas A-26 Airplane. NACA ARR No. L5H11a, 1946.
3. Goett, Harry J., Jackson, Roy P., and Belsley, Steven E.: Wind-Tunnel Procedure for Determination of Critical Stability and Control Characteristics of Airplanes. NACA ARR No. 4D29, 1944.

TABLE I.— GENERAL CHARACTERISTICS, DOUGLAS BTD-1 AIRPLANE

Manufacturer	Douglas Aircraft Co.
Type	Navy BTD-1
Navy number	04968
Normal gross weight	17,970 lb
Center-of-gravity locations	
Most forward allowable, gear-down	0.21 M.A.C.
Most rearward allowable, gear-up	0.29 M.A.C.
Maximum load factors	
17,000-pound gross weight	5.9g
18,000-pound gross weight	5.5g
Engines	
Make and type	Wright Duplex Cyclone R-3350-14, 14-cylinder double-row, one-speed supercharger, air-cooled
Propeller gear ratio	0.5625
Maximum speed limit	2800 rpm
Supercharger gear ratios	6.08 = 1, 8.52 = 1
Propeller	
Make and type	Curtiss Electric, constant-speed blade number X836-1C2-24
Number of blades	four
Diameter	12.67 ft

TABLE II.-- WING AND HORIZONTAL-TAIL-PLANE DIMENSIONS,
DOUGLAS BTD-1 AIRPLANE

Item	Wing	Horizontal tail
Area	¹ 391.5 sq ft	² 86.53 sq ft
Span	47.95 ft	19.85 ft
Aspect ratio	5.87	4.55
Taper ratio	0.469	0.506
Dihedral of leading edge	inner section -10° outer section 10°	7°
Incidence at root	$2^{\circ}1'51''$	1°
Root section	ESXX25-218	NACA 0012-64
Joint section	Modified NACA 65, 2-2518	-----
Tip section	NACA 65, 2-2515	Modified 10714
M.A.C.	8.56 ft	4.56 ft

¹ includes flap area

² includes elevator area

TABLE III.— CONTROL AND FLAP SURFACE DIMENSIONS,
DOUGLAS BTD-1 AIRPLANE

Item	Elevator	Elevator tab	Flaps
Type	Sealed nose balance with vane	-----	Partial-span Douglas retractable vane
Area (Aft of hinge line both sides)	21.65 sq ft	3.15 sq ft	45.28 sq ft
Span (one side)	8.19 ft	4.01 ft	12.25 ft
Travel	Flaps up 9.45° down 20.95° up Flaps down 4.2° down 32.2° up	15.8° up 5.0° down	35.0°
M.A.C.	1.38 ft	-----	-----
Chord	Tip 15.2 in. Root 30.1 in.	Inner 5.3 in. Outer 4.1 in.	-----

FIGURE LEGENDS

Figure 1.— Douglas BTD-1 airplane as instrumented for flight tests.
(a) Three-quarter front view, flaps retracted.

Figure 1.— Continued. Douglas BTD-1 airplane. (b) Three-quarter rear view, flaps extended.

Figure 1.— Concluded. Douglas BTD-1 airplane. (c) Rear view of horizontal stabilizer, showing elevator slat.

Figure 2.— Three-view drawing Douglas BTD-1 airplane.

Figure 3.— Detail of horizontal tail on the Douglas BTD-1 airplane.

Figure 4.— Variation of elevator control force with elevator angle as measured on the ground with no load on the control surfaces. Douglas BTD-1 airplane.

Figure 5.— Variation of elevator angle with stick position. Calibrated on the ground with no load on the control surfaces. Douglas BTD-1 airplane.

Figure 6.— The $3/16$ -scale model of the Douglas BTD-1 airplane as tested in the 7- by 10-foot wind tunnel. (a) Three-quarter rear view with the flaps and gear extended.

Figure 6.— Concluded. Douglas BTD-1 airplane. (b) Front view with the flaps and gear extended, in the presence of a ground board.

Figure 7.— Detailed view of extended flaps on the $3/16$ -scale model of the Douglas BTD-1 airplane.

Figure 8.— Variation of elevator control force and elevator angle with correct indicated airspeed. Glide condition, Douglas BTD-1 airplane.

Figure 9.— Variation of elevator control force and elevator angle with correct indicated airspeed. Power-on clean condition, Douglas BTD-1 airplane.

Figure 10.— Variation of elevator control force and elevator angle with correct indicated airspeed. Landing condition, Douglas BTD-1 airplane.

Figure 11.— Variation of elevator control force and elevator angle with correct indicated airspeed. Approach condition, Douglas BTD-1 airplane.

Figure 12.— Variation of elevator angle with lift coefficient. Landing condition, Douglas BTD-1 airplane.

Figure 13.-- Variation of neutral point with correct indicated
airspeed. Douglas BTD-1 airplane. (a) Flap and gear up.

Figure 13.-- Concluded. Douglas BTD-1 airplane. (b) Flap and gear
down.

Figure 14.-- Variation of tab effectiveness with lift coefficient.
Douglas BTD-1 airplane.

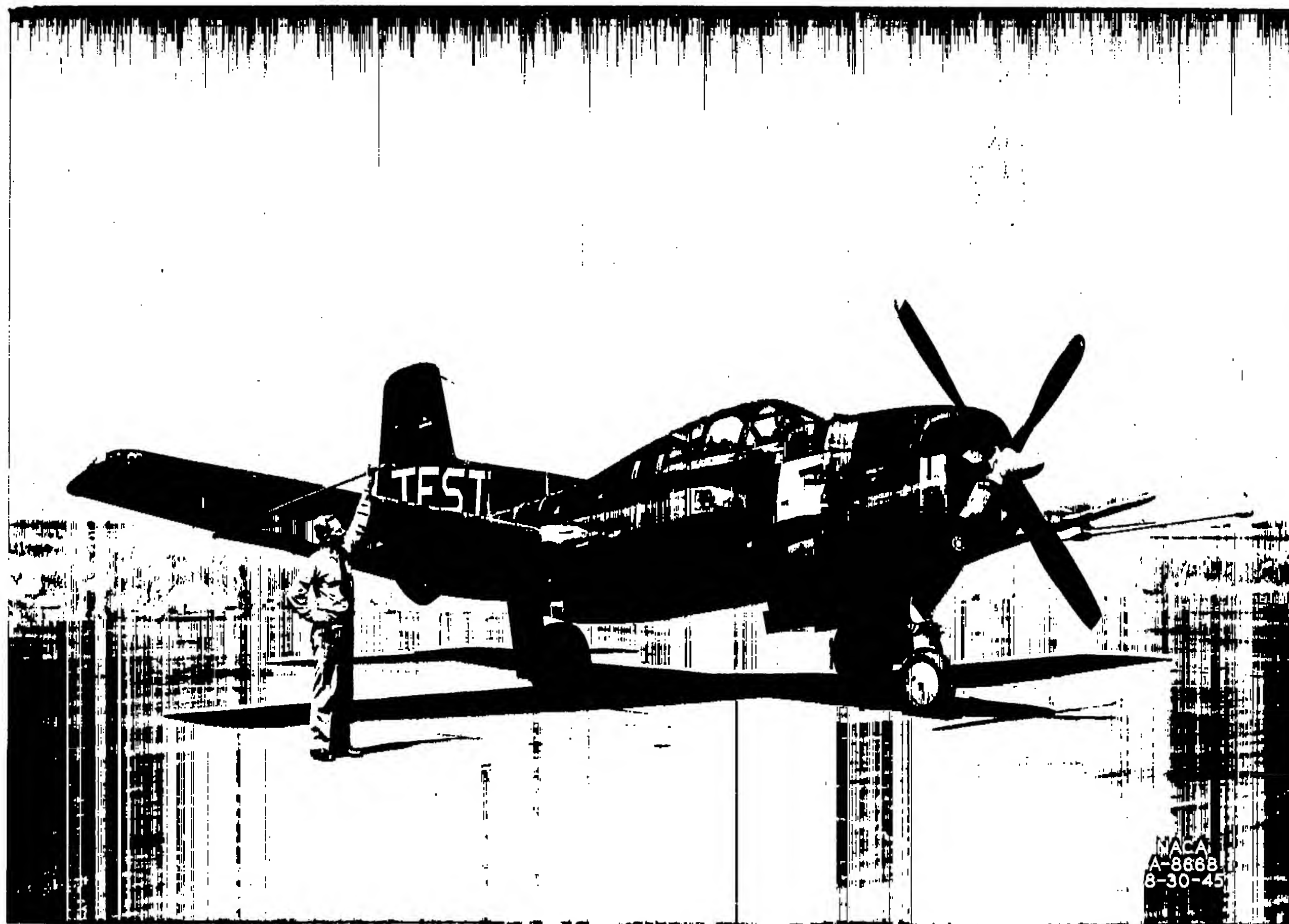
Figure 15.-- Variation of elevator control force and elevator angle
with normal acceleration in steady turns. Power-on clean,
Douglas BTD-1 airplane.

Figure 15.-- Continued. Douglas BTD-1 airplane.

Figure 15.-- Concluded. Douglas BTD-1 airplane.

Figure 16.-- Variation of elevator control-force gradient with
center-of-gravity position. Power-on clean condition, Douglas
BTD-1 airplane.

Figure 17.-- Variation of elevator angle and control force with
contact airspeed in landings. Douglas BTD-1 airplane.

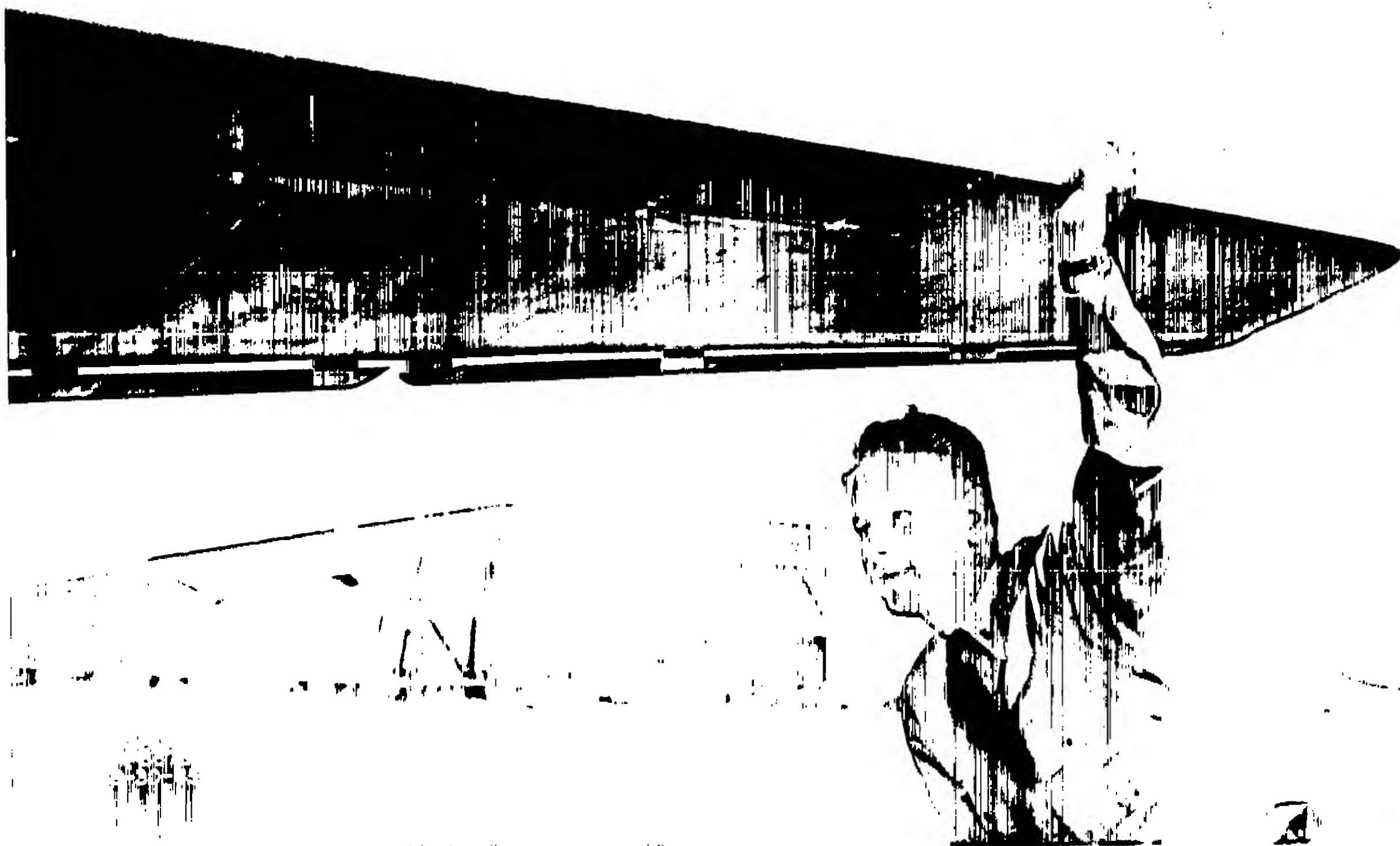


(a) Three-quarter front view, flaps retracted.

Figure 1.- Douglas BTD-1 airplane as instrumented for flight tests.



(b) Three-quarter rear view, flaps extended.
Figure 1.- Continued. Douglas BTD-1 airplane.



(c) Rear view of horizontal stabilizer, showing elevator slat.

Figure 1.- Concluded. Douglas BTD-1 airplane.

NAVAL AIR 16130

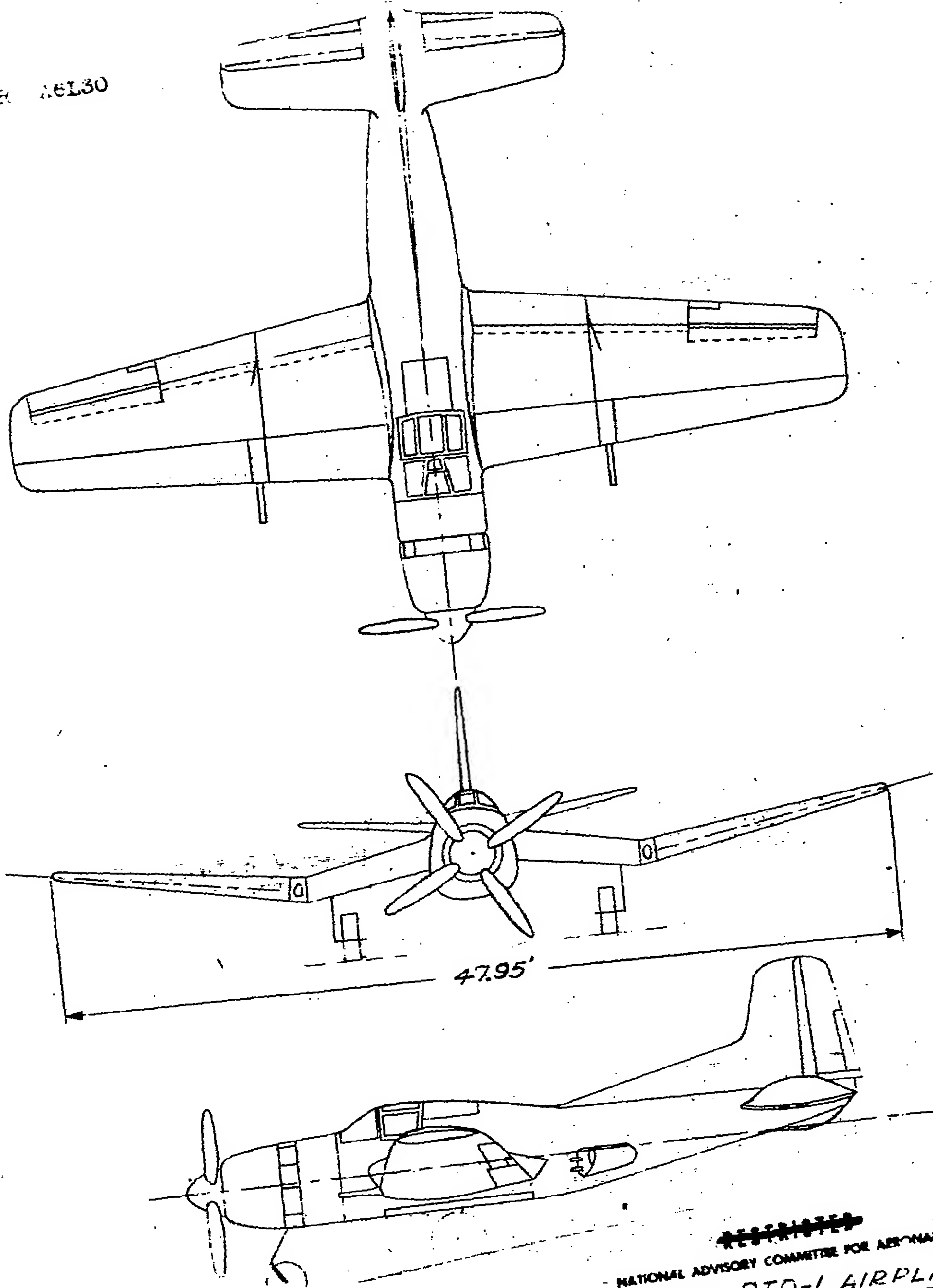
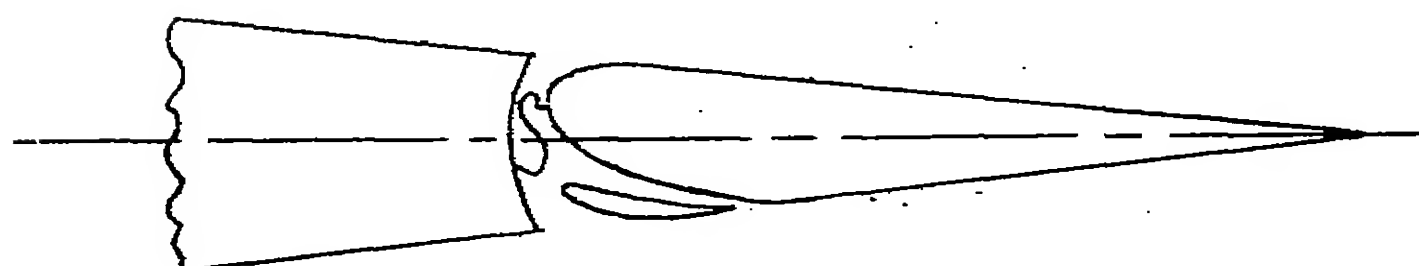
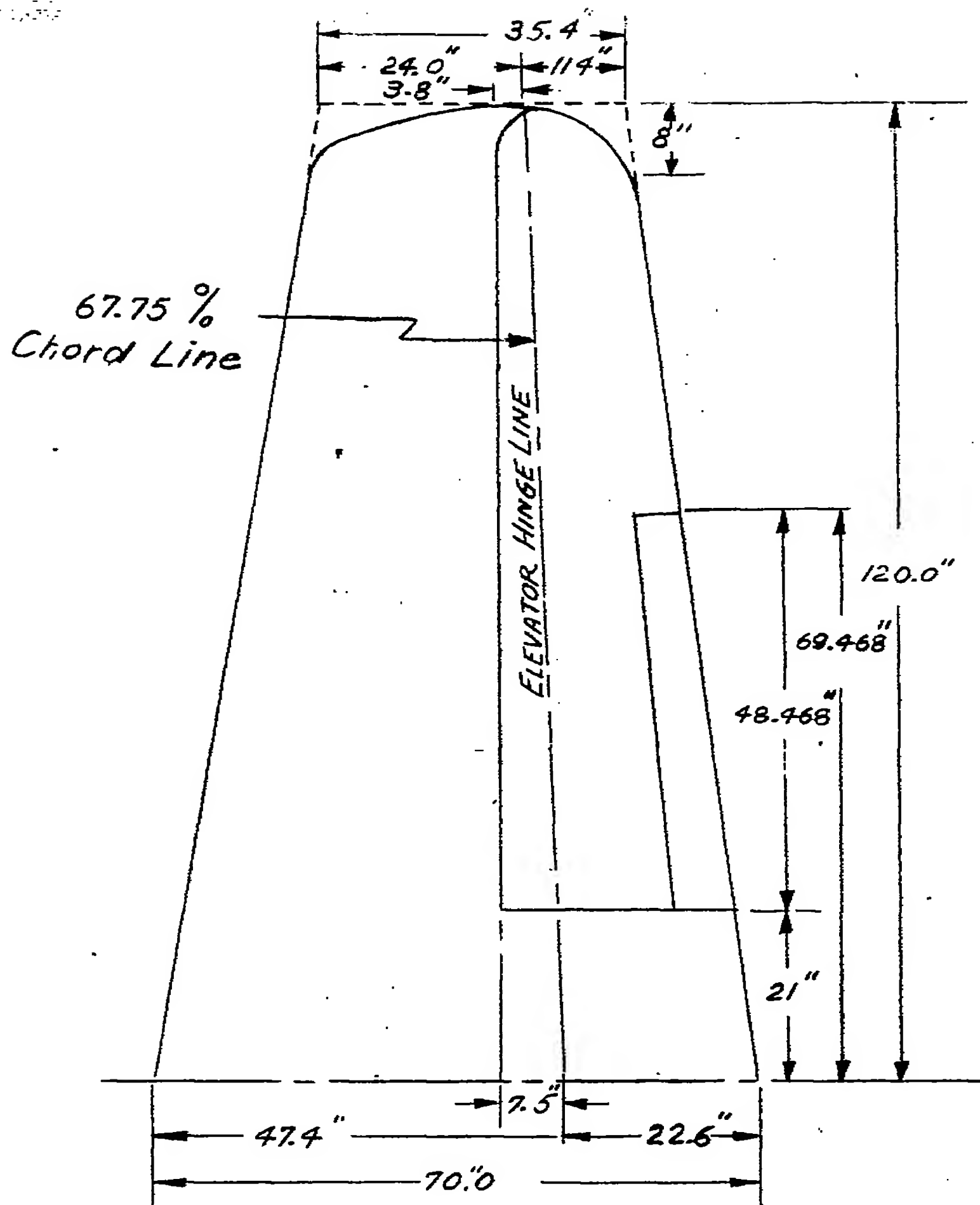


FIGURE 2. - THREE-VIEW DRAWING DOUGLAS BTD-1 AIRPLANE

NATIONAL ADVISORY COMMITTEE FOR AERONAUTICS



TYPICAL SECTION

~~RESTRICTED~~

NATIONAL ADVISORY COMMITTEE FOR AERONAUTICS

FIGURE 3 — DETAIL OF HORIZONTAL TAIL ON THE
DOUGLAS BTD-1 AIRPLANE

Elevator control force, lb pull

20

0

8

4

0

4

8

12

down

up

Elevator angle, deg

Friction

slow movement

slow movement

Spring

Figure 4.—Variation of elevator control force with elevator angle as measured on the ground with no load on the control surfaces. Douglas BTD-1 airplane.

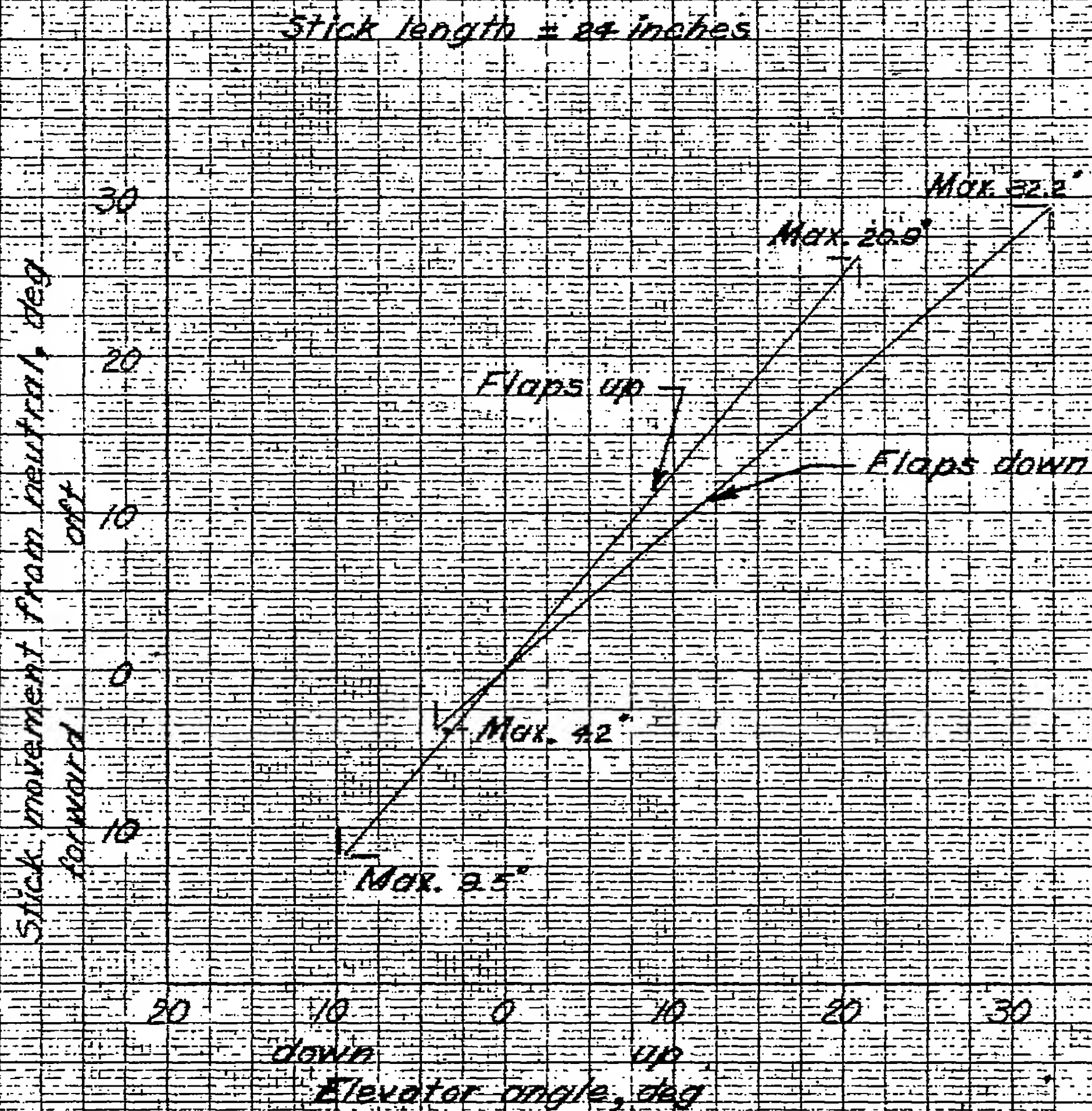
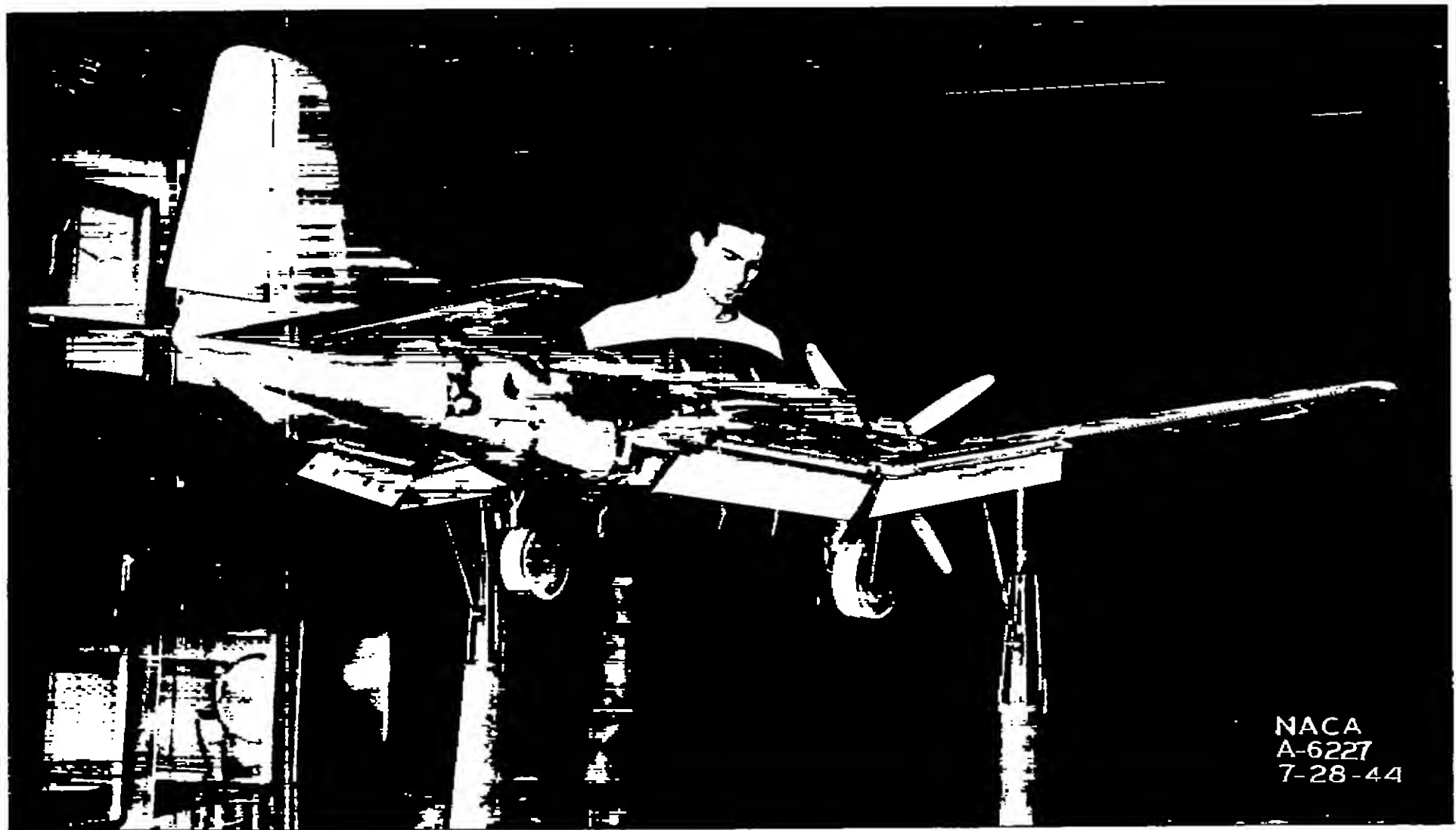
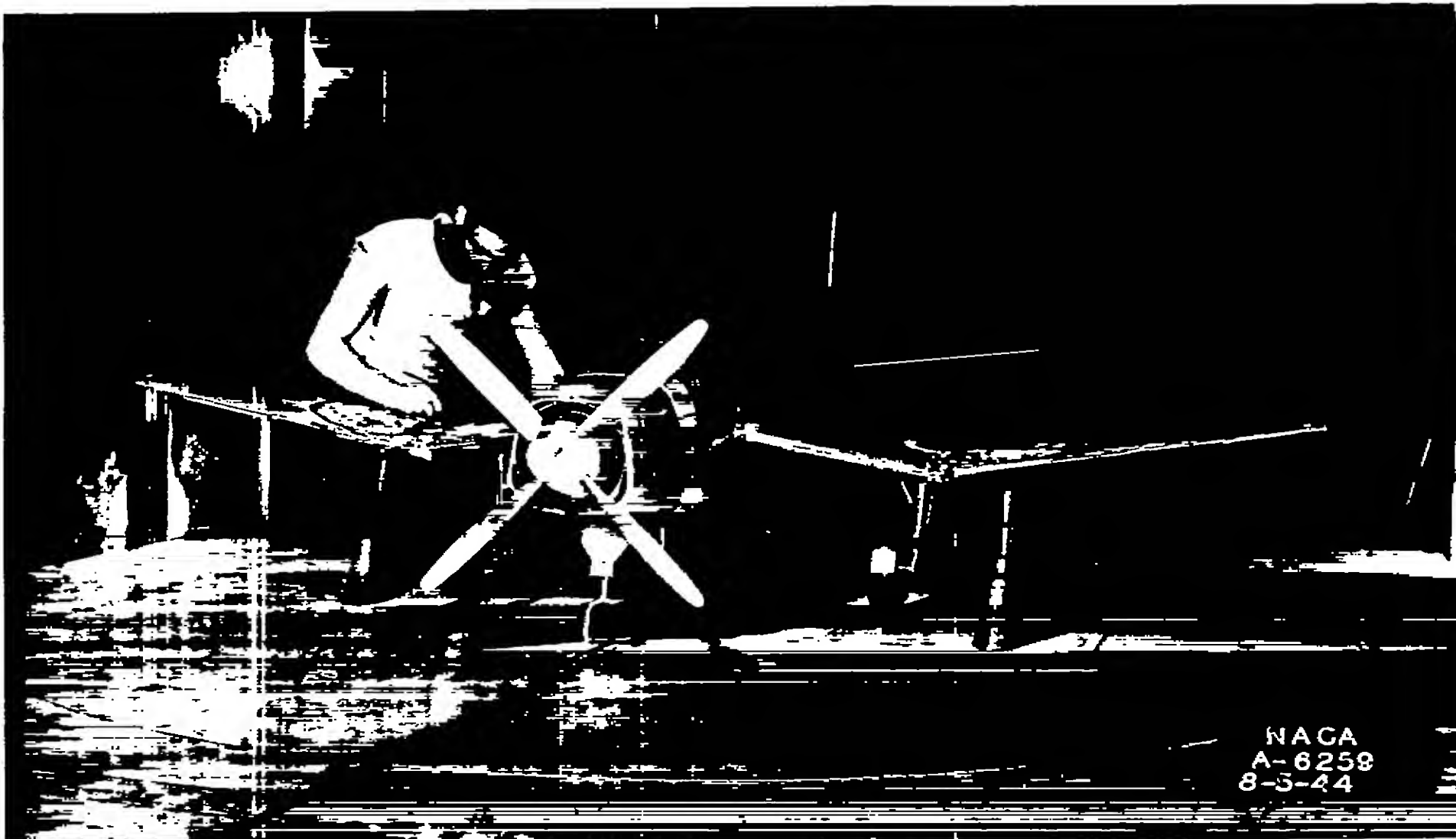


Figure 5 - Variation of elevator angle with stick position. Calibrated on the ground with no load on the control surfaces. Douglas BTD-1 airplane.



(a) Three-quarter rear view with the flaps and gear extended.

Figure 6.— The 3/16-scale model of the Douglas BTD-1 airplane as tested in the 7- by 10-foot wind tunnel.



(b) Front view with the flaps and gear extended, in the presence of a ground board.

Figure 6.— Concluded. Douglas BTD-1 airplane.

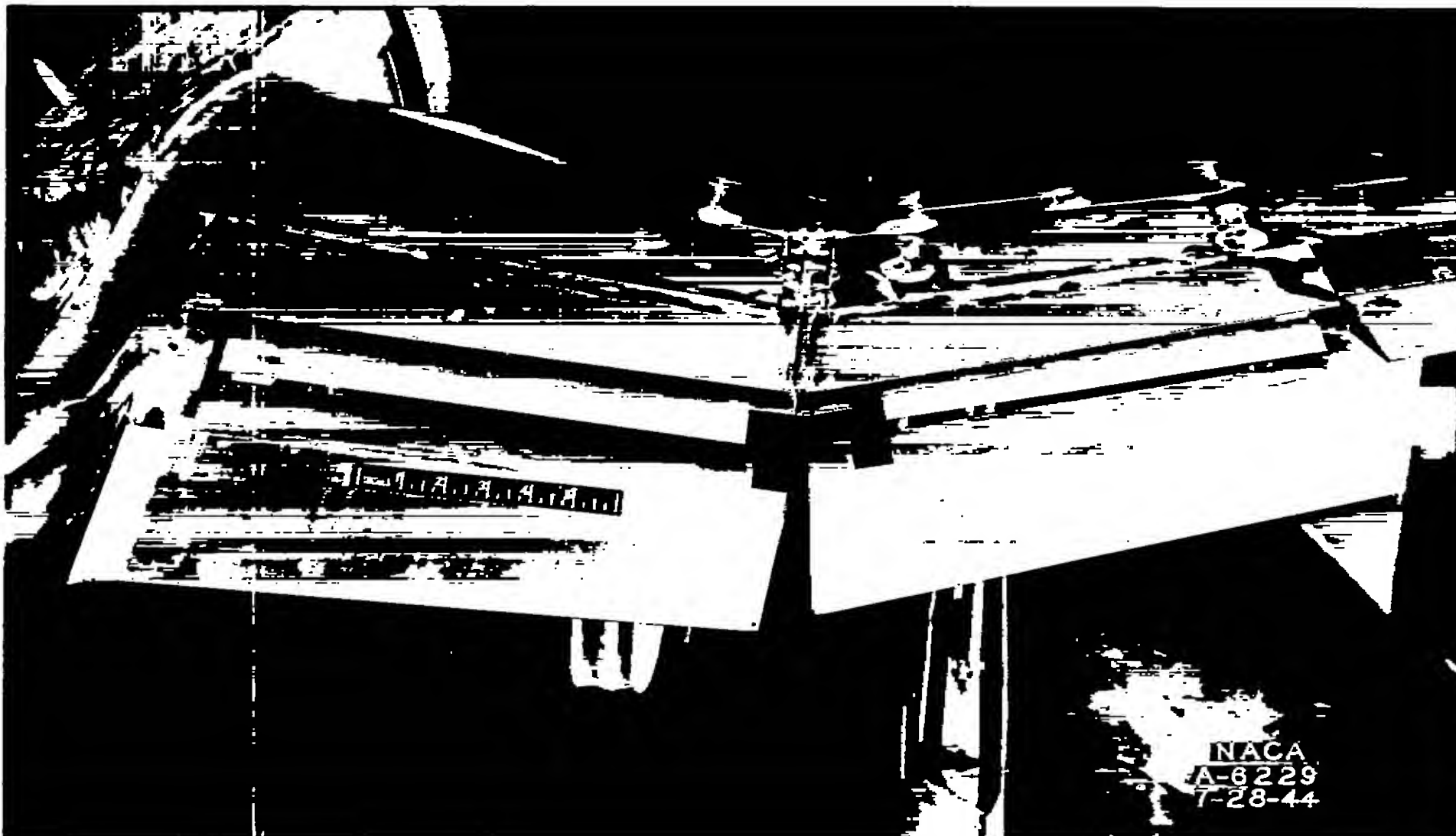
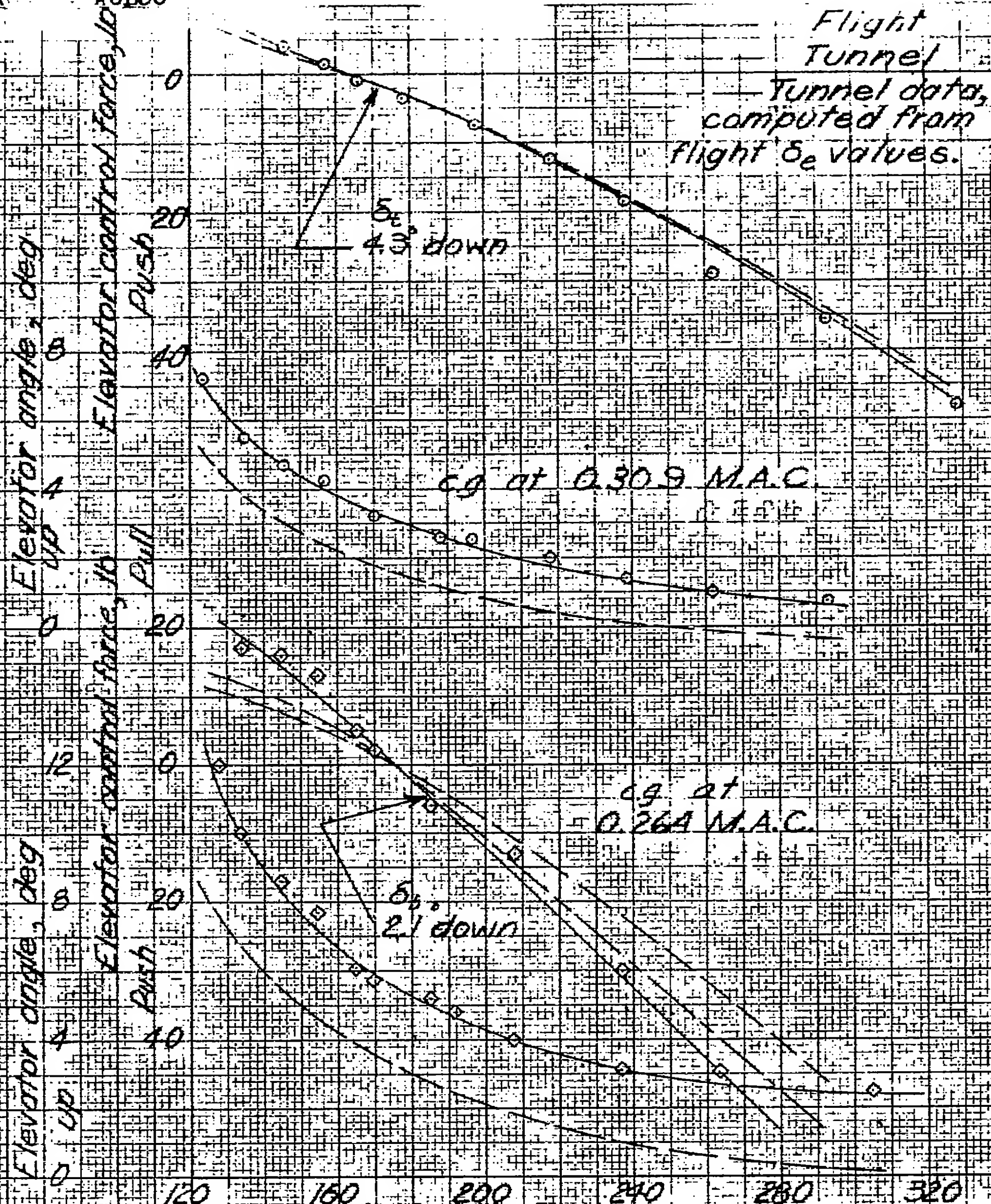


Figure 7.— Detailed view of extended flaps on the 3/16-scale model of the Douglas BTD-1 airplane.



Correct indicated airspeed, mph

Figure 8 - Variation of elevator control force and elevator angle with correct indicated airspeed. Glide condition; Douglas BTD-1 airplane.

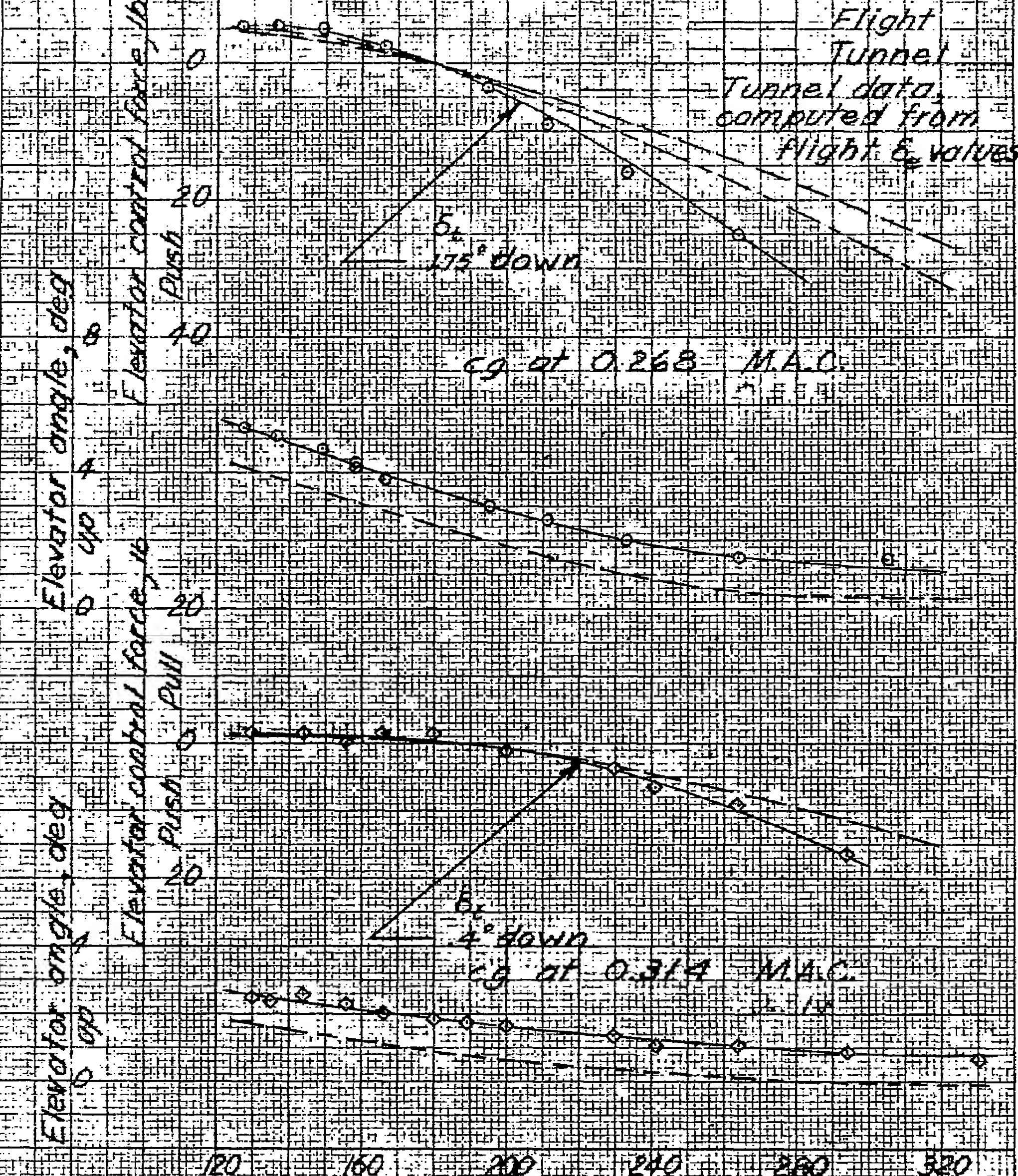


Figure 9 - Variation of elevator control force and elevator angle with correct indicated airspeed. Power on clean condition, Douglas BTD-1 airplane.

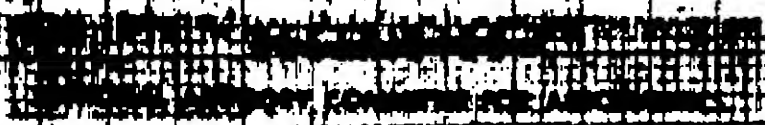


Figure 10-Variation of elevator control force and elevator angle with correct indicated airspeed. Landing condition, Douglas BTD-1 airplane.



Figure 11 - Variation of elevator control force and elevator angle with correct indicated airspeed. Approach condition, Douglas B-1 airplane.

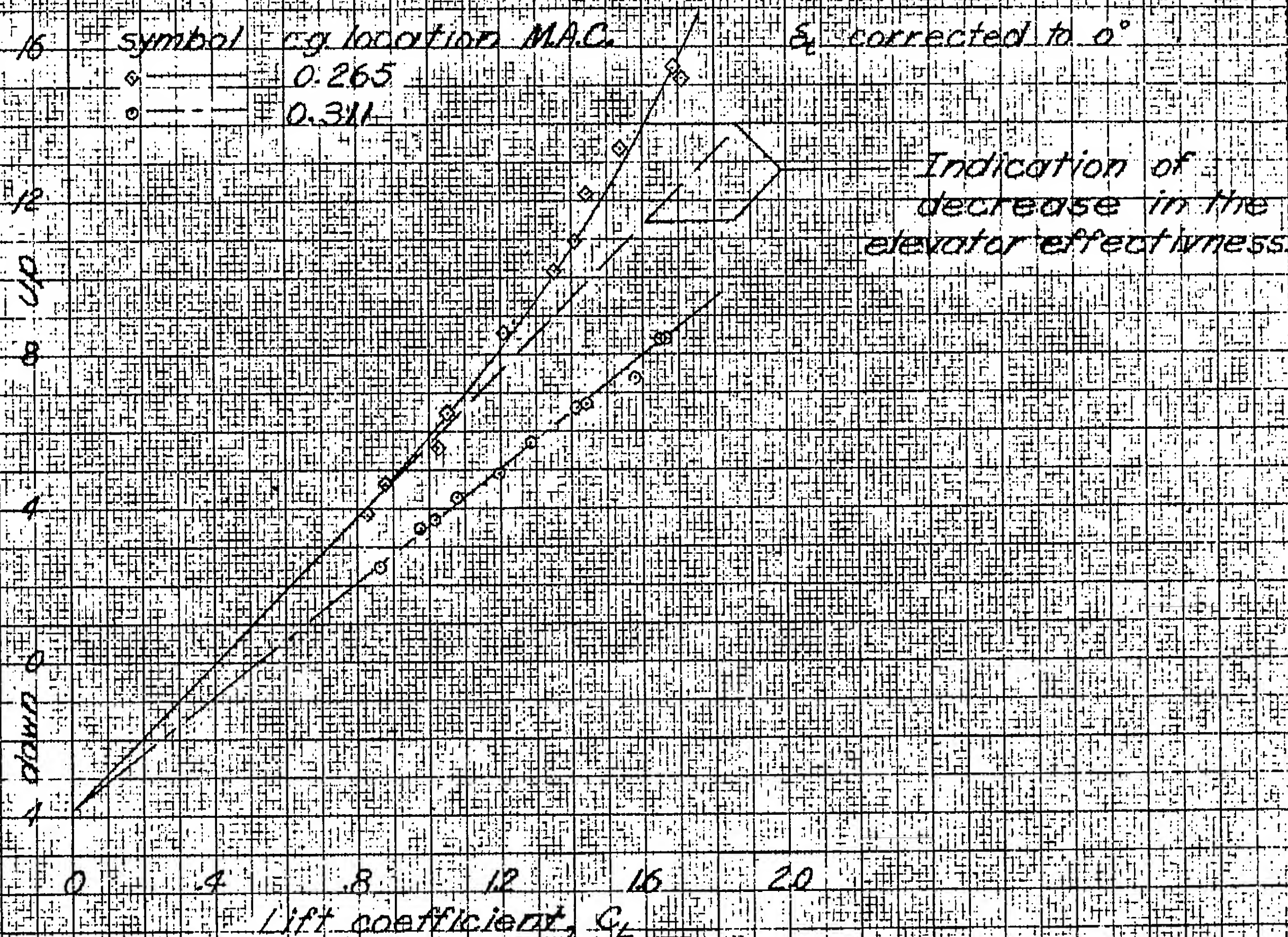


Figure 12- Variation of elevator angle with lift coefficient.
 Landing condition, Douglas BTD-1 airplane.

Glide Condition

Stick Fixed

Stick Free

Flight
Tunnel

Power-on clean Condition

Stick Fixed

Stick Free

Neutral point, percent MAC

40

36

32

40

36

32

28

12 14 16 18 20

120

160

200

240

280

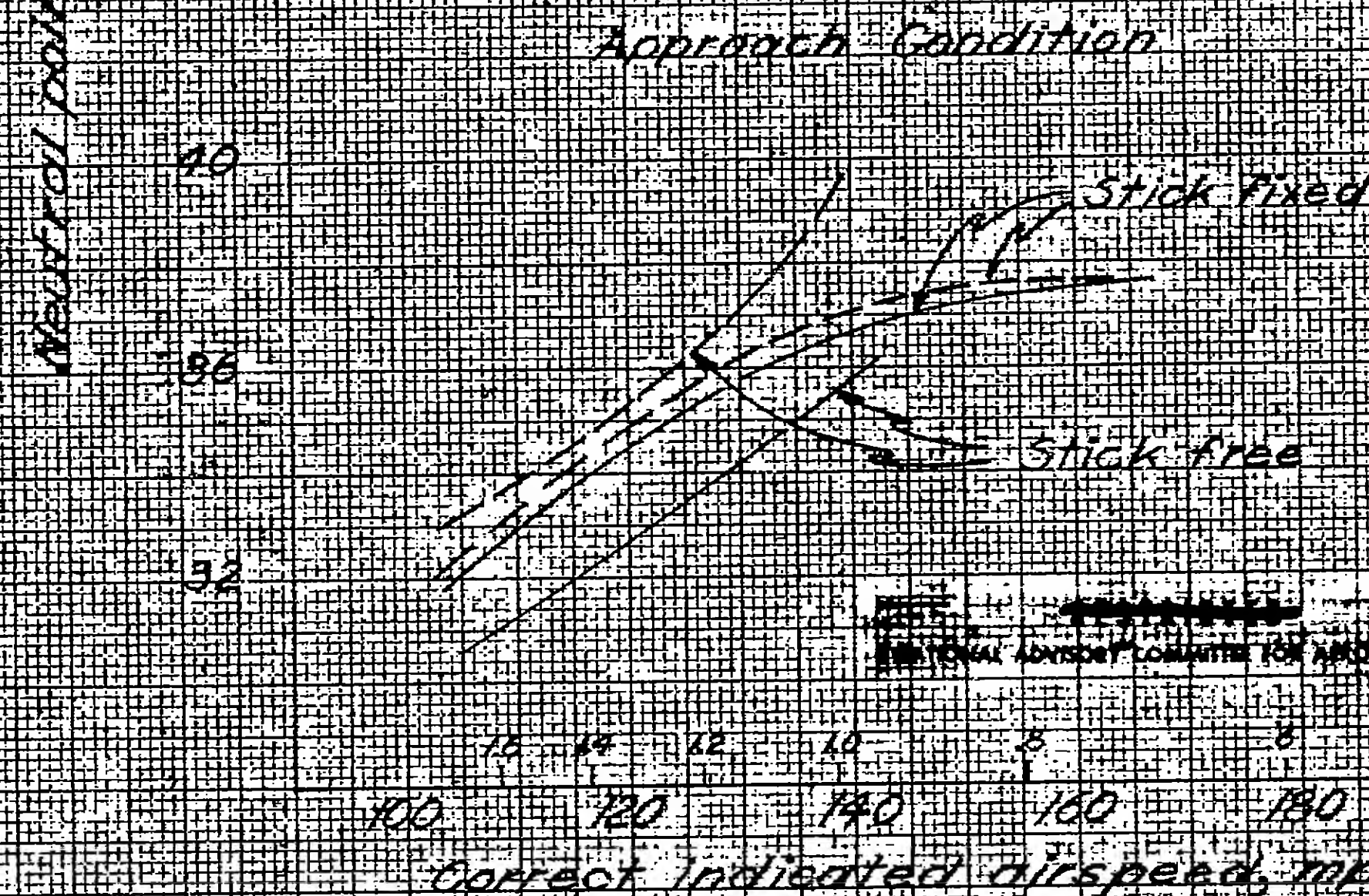
320

Correct indicated airspeed, mph

Flap and gear up

Figure B - Variation of neutral point with correct indicated airspeed Douglas BTD-1 airplane

RESTRICTED



(b) Flap and gear down
Figure 13 - concluded. Douglas BTD-Lampplane

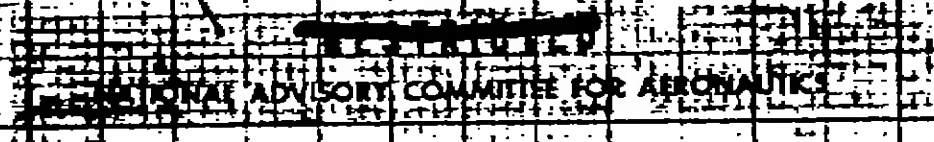


Figure 14 - Variation of tab effectiveness with lift coefficient. Douglas BTD-1 airplane.

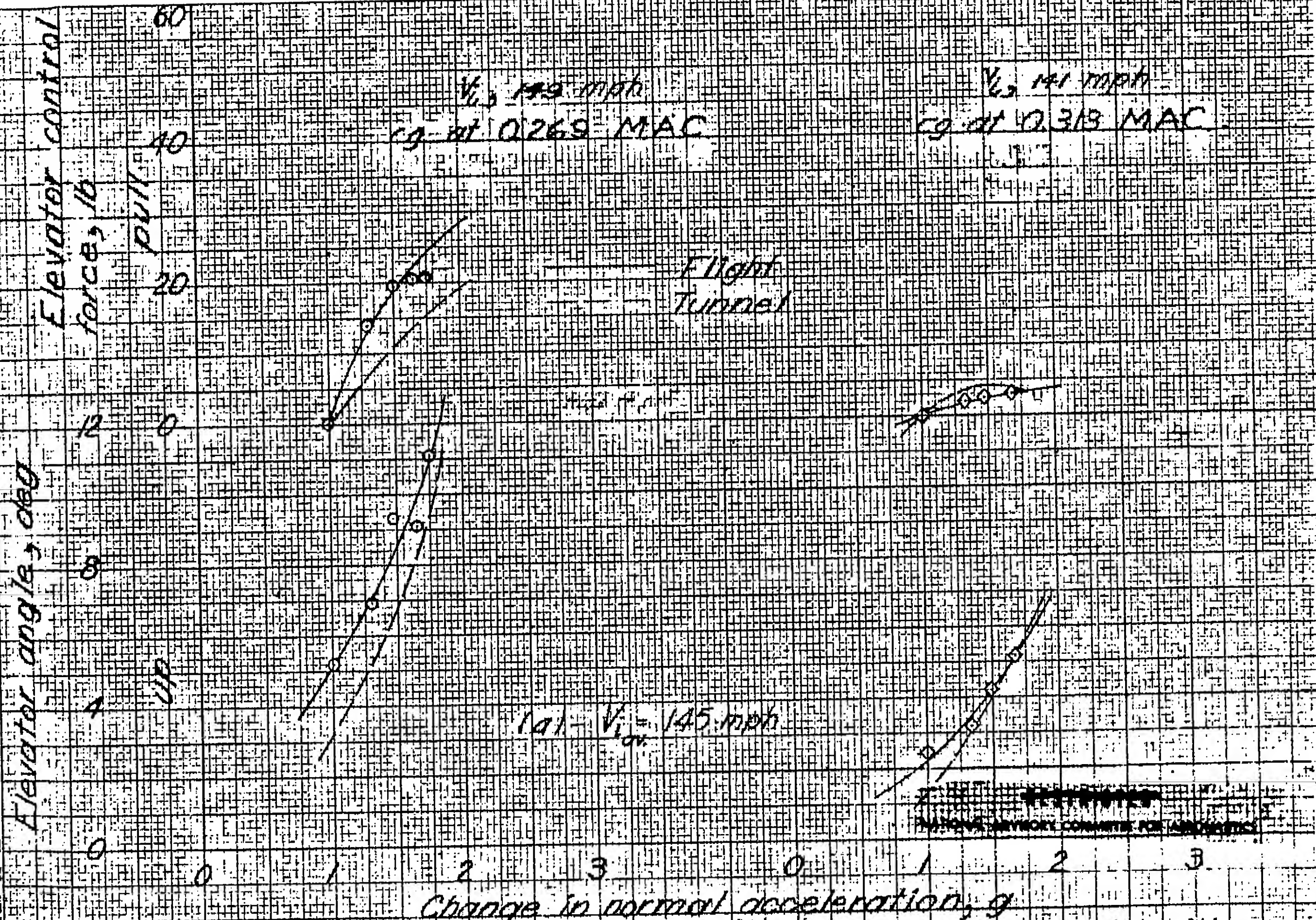


Figure 15- Variation of elevator control force and elevator angle with normal acceleration in steady turns. Power on clean, Douglas BTD-1 airplane

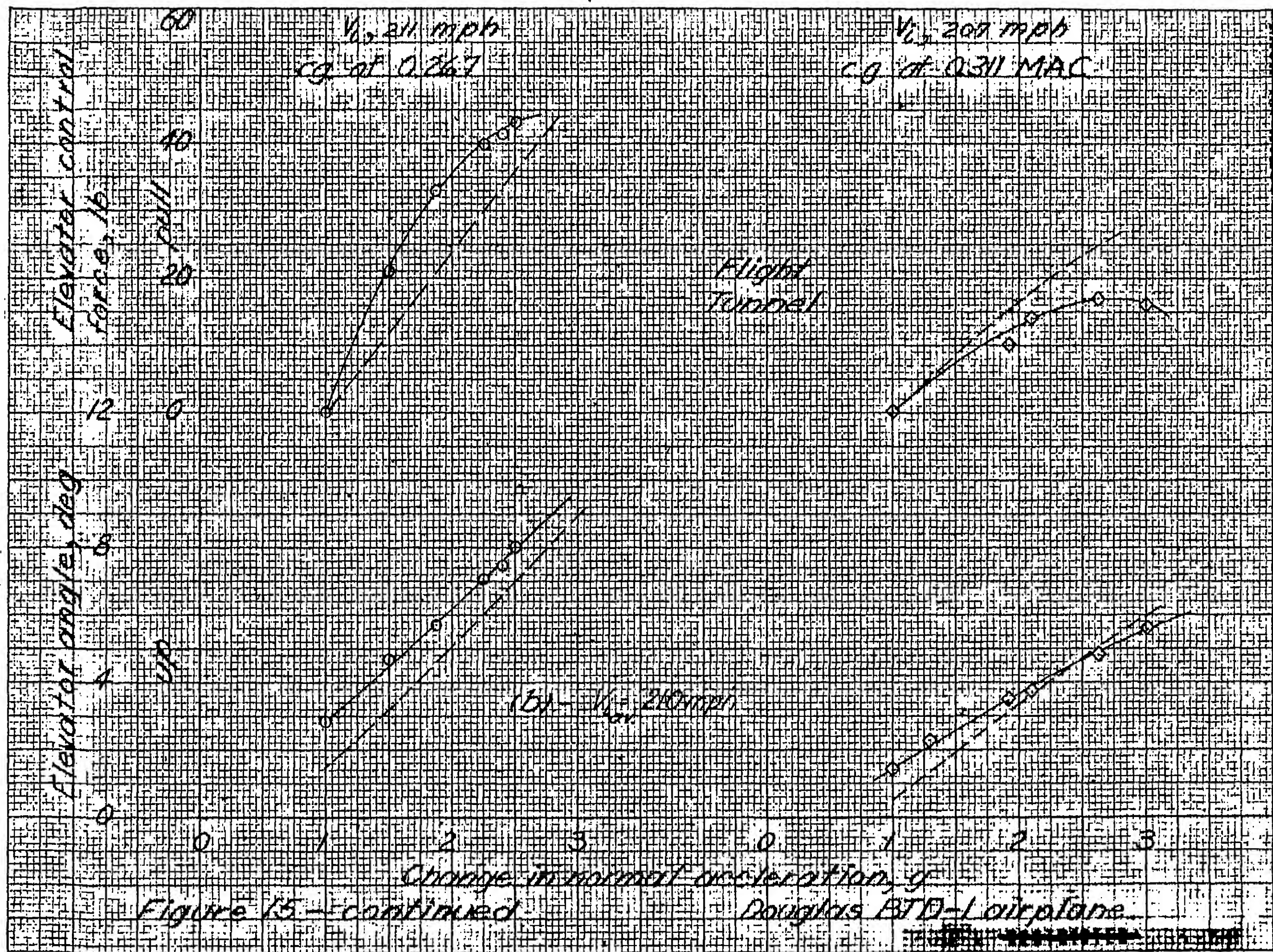
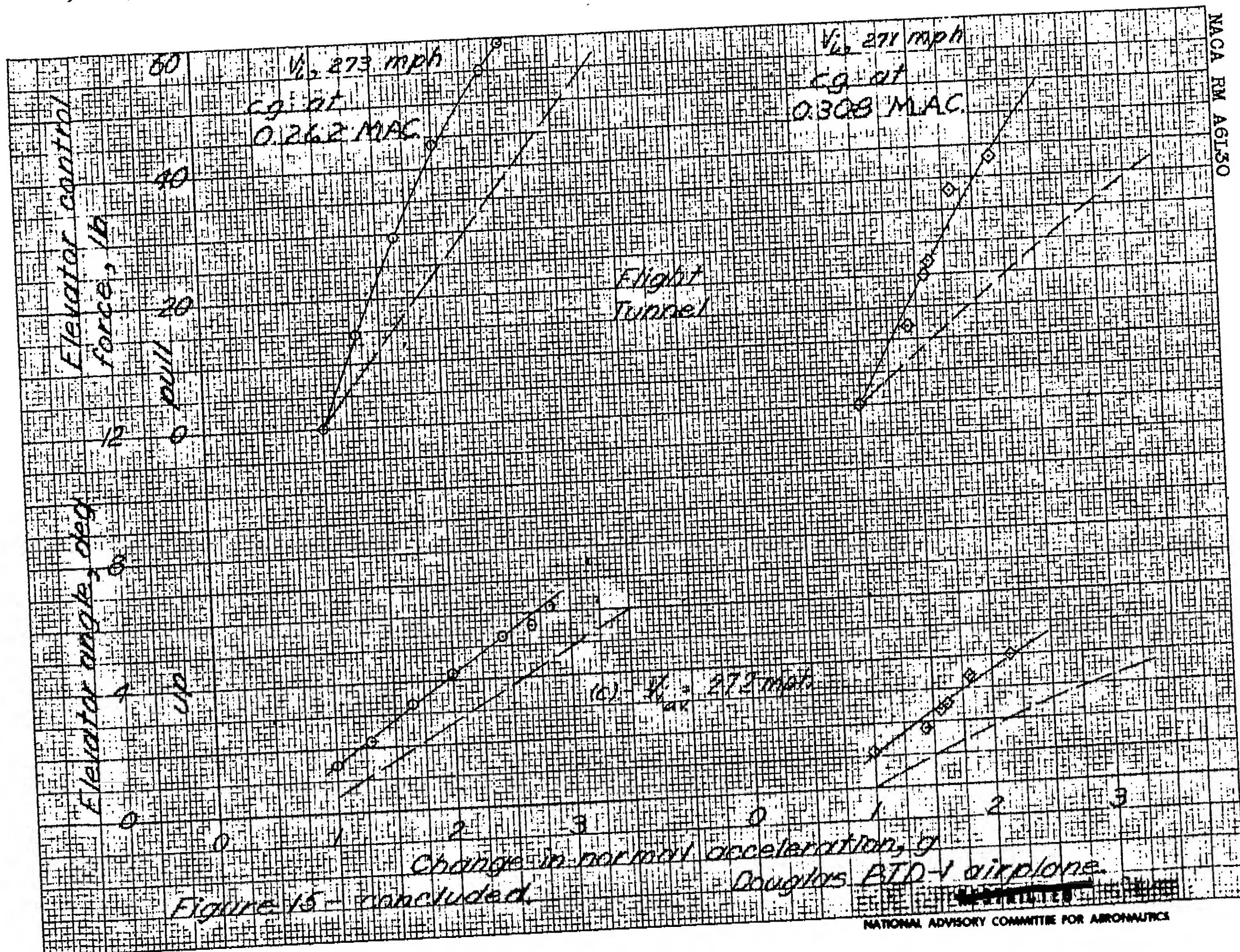
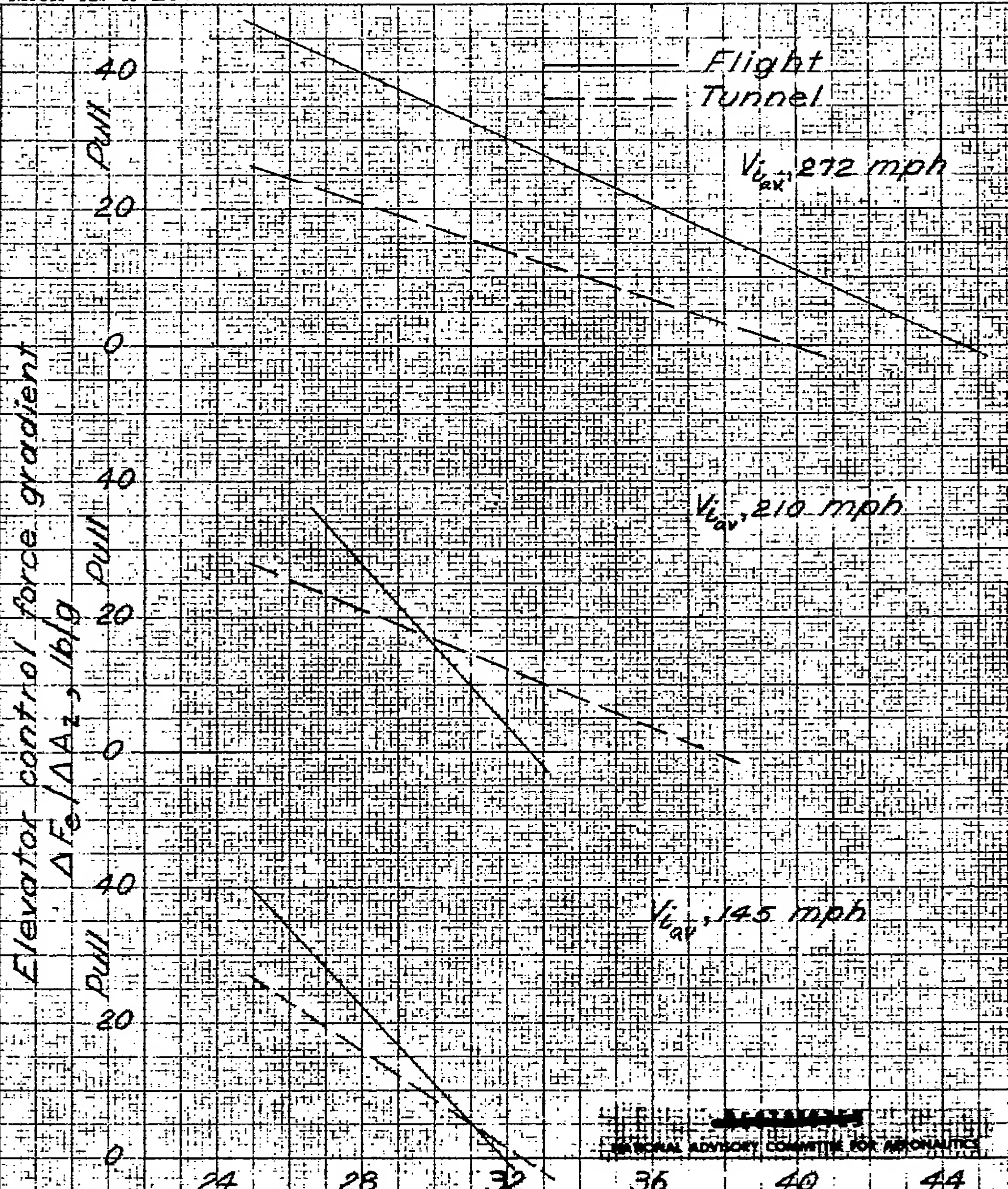


Figure 15 - continued

Douglas BTD-1 Airplane





Center of gravity position, M.A.C.
 Figure 16-Variation of elevator control-force gradient with center-of-gravity position. Power-on clean condition, Douglas BTD-1 airplane.

Elevator angle, deg

up

Elevator control force, lbs pull

26

22

18

14

60

40

20

90

100

110

120

130

Correct indicated airspeed, mph

Flight Tunnel

C.G. at 0.263 M.A.C.

6° 2.5° down
1° down

C.G. at 0.316 M.A.C.

C.G. at 0.263 M.A.C.

C.G. at 0.316 M.A.C.

Figure 17 - Variation of elevator angle and control force with correct airspeed in landings, Douglas BTD-1 airplane.